REFLECTOMETERS, TIME-DOMAIN

INTRODUCTION

Time-domain reflectometry is a measurement technique applied to determine the location, type, and quantitative character of discontinuities distributed in signal transmission channels such as computer or telephone networks, printed circuit boards, or other systems where signal delays are observed. Testing such systems, called *devices under test* (DUT), with TDR involves use of a fast pulse generator along with a *sampling oscilloscope* (11) and test fixture. Signals generated by the pulse generator are sent through the test fixture to the DUT. The most popular testing signal generated in broadband TDR systems is a step-like voltage. The signals are registered at the input to the *test fixture* by means of a sampling oscilloscope with coherent sampling, time transformation, and a track-and-hold vertical deflection system. Such a device allows the display of very small levels of reflected signals on the top of high levels of applied signals with minimal distortion.

TDR techniques can be enhanced when not only the input terminals of the DUT but also the output terminals are accessible by the oscilloscope. Measurements made from the output terminals, often called time-domain transmission (TDT) tests, include propagation delay and a pulse transmission function. Transmission tests can also show the effects of mutual coupling between adjacent transmission channels, such as printed circuit board (PCB) traces.

In the article, the TDR measurement techniques are described, including basic properties and limitations of a real system such as finite risetime of the pulses, smooth transitions, small overshoots, jitter, and noise. Major examples demonstrated here include tests of the following:

- Resistance
- Capacitance
- Inductance
- Transmission-line characteristic impedance
- Inserted discontinuities of inductive, capacitive, and mixed types
- Differential and common-mode transmission-line impedances

In addition, effects of *transmission-line losses* and processes for correcting TDR test channel distortions are described. SPICE simulations are frequently used in conjunction with TDR measurements to enhance identification of characteristics related to the discontinuities (10–15). The results of PSPICE simulations, included here to illustrate the normalization processes, are based on a demonstration version of this program (16). The last part of the article demonstrates practical applications of TDR/TDT systems (3–17).

Applications of Time-Domain Reflectometry/Time-Domain Transmission

TDR/TDT systems have found use in both electrical and nonelectrical areas. The following list includes a number of the most popular applications (1–12):

1. Conductor length and return loss determination
2. Finding short and open connections in cables
3. Location of bad splices, loose connectors, and crimps
4. Location of moisture and water in cables
5. Measurement of cable parameters, such as characteristic impedance, losses, and propagation velocity
6. Determining signal integrity, and performing failure analysis of printed circuit boards used in high-speed digital and analog circuits
7. Evaluation of microstrip connections
8. Computer network cable tests
9. Characterization of integrated circuit packages
10. Sensing liquid levels

TIME-DOMAIN REFLECTOMETRY PRINCIPLES

Basic TDR/TDT Systems

A functional block diagram of a TDR/TDT is shown in Fig. 1. The step generator signal is transmitted through a test fixture such as transmission line (Fig. 2), and is finally applied to the device or system under test (DUT). The test fixture impedance is usually matched to that of the generator. If the DUT impedance is not equal to the *characteristic impedance* of the transmission line of the test fixture, part of the incident voltage is reflected from the DUT. The reflected signal, which is delayed in relation to the incident voltage, appears as a step change on top of the incident wave. The location of the *impedance discontinuity d* can be calculated from the transit time measured from the reflection and the reference point, marked from the front edge of the incident voltage signal

$$d = \frac{v_p \cdot t_d}{2} \tag{1}$$

where v_{p} is a wave propagation velocity and t_{d} is the transit time.

Figure 3 shows the voltages observed in a TDR/TDT system when the transmission line of the test fixture is matched to the source and the signals are reflected from pure resistive loads. The voltage amplitude reflected from the DUT, divided by the amplitude of the incident wave, determines the reflection coefficient at the load ρ_{L}. When an unknown resistance is connected to the source-matched transmission line, the value of the resistance can be calculated as follows:

$$Z_{\mathrm{L}} = Z_0\left(\frac{1+\rho_{\mathrm{L}}}{1-\rho_{\mathrm{L}}}\right) \tag{2}$$

This equation is applied in the TDR/TDT internal processor to calculate the load parameters (15, 16) (see also PSPICE simulations of differential TDR/TDT, Figs. 15,17). Figures 4-7 illustrate the voltage waveforms when the load of the

J. Webster (ed.), *Wiley Encyclopedia of Electrical and Electronics Engineering*. Copyright © 2007 John Wiley & Sons, Inc.

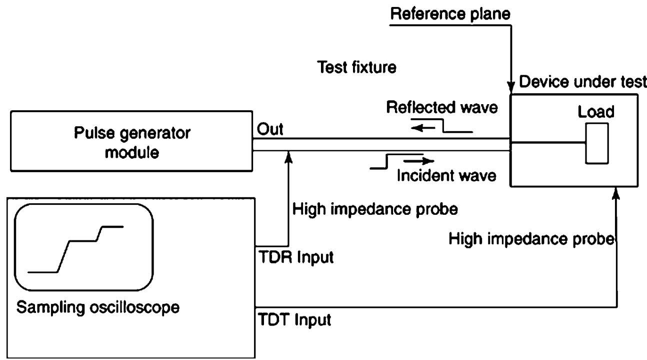

Figure 1. Block diagram of a time-domain reflectometer with time-domain transmission.

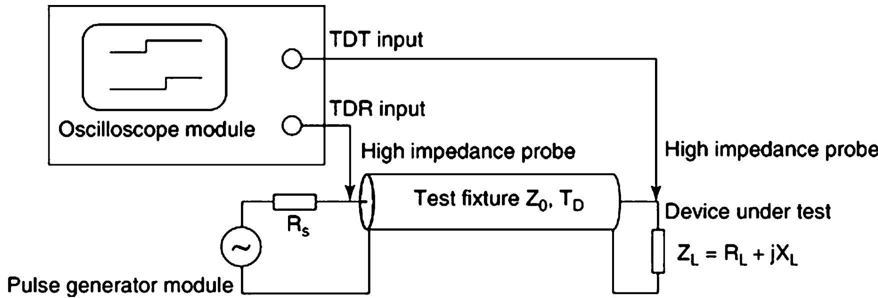

Figure 2. Impedance tests with a 50-Ω transmission-line test fixture.

test fixture (transmission line) is a combination of either resistance and capacitance, or resistance and inductance. In all cases shown, the load resistance is varied and either C or L is maintained constant. From steady-state voltage levels following the reflection, as well as from the shapes of the waves themselves, which reveal the time constant, it is possible to identify the character of the load and the values of unknown components. With this information, the parameters of the equivalent circuits representing the load can be evaluated from the equations listed in Table 1.

The waves that have been presented so far show the behavior of short transmission lines in which the losses, which are due largely to the skin effect, are negligible. In longer transmission lines the distributed losses distort the signals traveling along the lines. Examples of transmitted and reflected waves in a short terminated transmission line are shown in Fig. 8. For comparison, a lossless case is included. From these waveforms, it is possible to determine changes of the transmission-line resistance over the length of the cable.

Practical transmission channels in PCBs with packages of the integrated circuits may have longer connecting leads inserted between some sections of transmission lines or larger conductive surfaces shunting the signal. The TDR/TDT tests for such cases can be modeled as shown in Fig. 9. Two examples of the waveforms in these circuits are illustrated in Figs. 10 and 11.

Sources of Error

Three major sources of error are encountered in TDR/TDT tests:

1. Cables and connectors of the test fixture (2–7).
2. Oscilloscope
3. Test generator

Cables and connectors connecting the generator with the tested device introduce their own *reflections*, in addition to the reflections caused by the tested device (DUT). They also introduce distributed losses, which increase at higher frequencies. This reduces the speed of transition of generator pulses.

Oscilloscopes introduce two types of error. One is caused by bandwidth limitation, which leads to the “smoothing” of fast voltage transitions. The other type of errors includes coupling of the trigger channel into signal channel, interchannel interference, and input circuit mismatches to the test fixture (2–7).

Real testing pulses of TDR/TDT pulse generators have finite risetimes, and their top parts are not ideally flat. Some generators may produce pulses with overshoots. Associated with both the sampling oscilloscope and the generator are the errors caused by both jitter and noise. All these distortions limit TDR/TDT system resolution and make the observed waves more difficult to analyze, especially when the TDR/TDT system is used to test closely located small discontinuities of the transmission channel.

Corrections of Measurement Errors

Error correction can be effectively performed using internal signal processors built into modern TDR/TDT systems. One of the simplest methods of error correction is waveform subtraction. The method could be used to minimize errors common to both the tested device and the reference, such as trigger and *channel crosstalk errors*, and reflections from the test fixture and connectors. In the process of measurement, the common reference device is connected to the end of the test fixture. The test results in terms of the TDR input voltage are stored and the reflected part of this wave is computed. This reflected wave is then subtracted from the input voltage obtained in the second phase of the measurements when the DUT is connected. The results of this pro-

Table 1. Parameters of Equivalent Circuits Representing Load in Basic TDR/TDT Systems

Voltage Level for $t \to \infty$	Circuit Time Constant
For parallel connection of R_L and C_L	
$V_{in}(\infty) = \frac{R_L}{R_L + R_S} V_{source}$	$\tau = \frac{R_L \cdot R_S}{R_L + R_S} C_L$
For series connection of R_L and C_L	
$V_{in}(\infty) = V_{source}$	$\tau = (R_L + R_S) C_L$
For parallel connection of R_L and L_L	
$V_{in}(\infty) = 0$	$\tau = \frac{L_L(R_S + R_L)}{R_S \cdot R_L}$
For series connection of R_L and L_L	
$V_{in}(\infty) = \frac{R_L}{R_L + R_S} V_{source}$	$\tau = \frac{L_L}{R_S + R_L}$

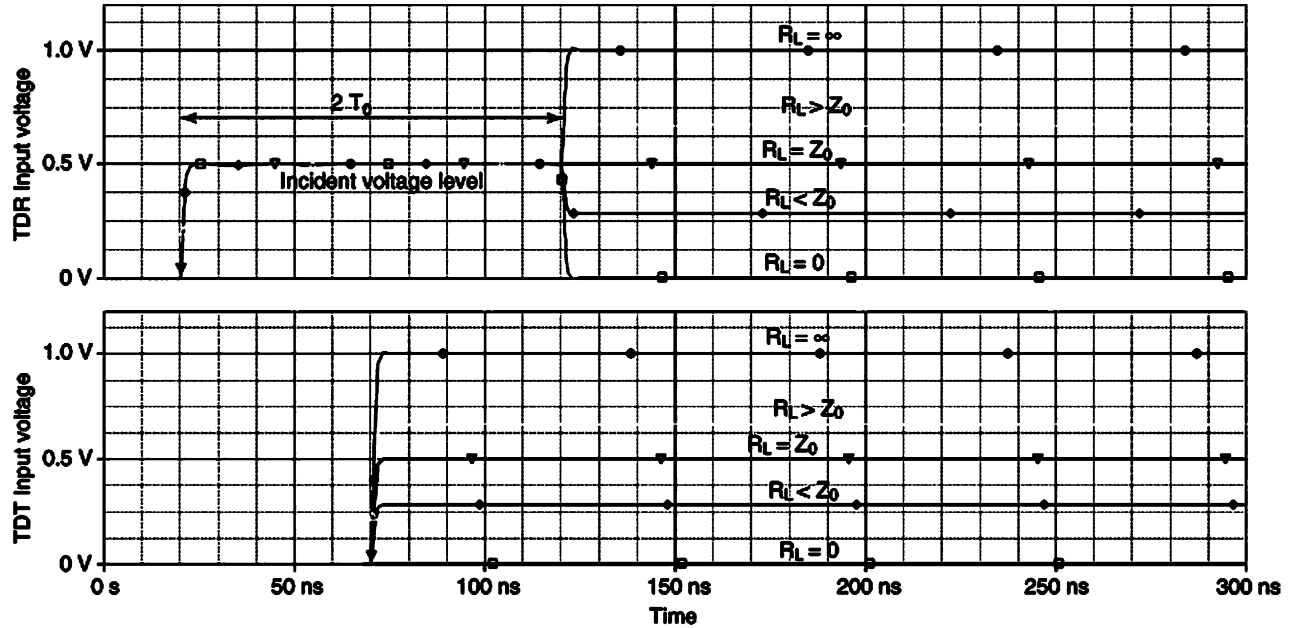

Figure 3. Displays demonstrating TDR and TDT input voltages for various resistances connected to a 50-Ω line test fixture.

cedure are limited to the specific risetime of the system. For instance, faster pulses reveal more discontinuities, which may not be important in particular applications.

The waveform subtraction method is illustrated by means of PSPICE (PSPICE is a PC version of SPICE) simulations. Figures 12 and 13 show the process of compensation for errors introduced by the test fixture composed of two transmission-line sections, T3 and T4. The characteristic impedances of these lines are 52 and 40 W, respectively. The device under test (DUT) is a connection of two transmission lines, two inductances and one resistor (L1, T5, T6, L2, and R6). Initially, the matching resistor (50 W) is connected to the end of the test fixture. Then, the calculated reflected waves are subtracted from the results of final tests while the DUT is connected. In the simulations, the calculations are performed in a parallel manner so the 50-Ω tests are done internally, inside the processing box. When the test fixture reflections can be isolated in time from the DUT reflections, it is possible to process the latter signals by windowing and creating corresponding impedance profiles (16). It is still necessary to calibrate the test fixture with the reference device connected to the end of the test fixture as in the waveform subtraction method described earlier.

A significant reduction of the TDR/TDT system errors caused by the pulse generator speed limits can be achieved in a TDR/TDT system that takes advantage of digital signal processing called *normalization* (3, 4). The normalization process refers the measurement results to a test signal with a predefined risetime (5). The measurement results are enhanced by digital filtering to boost high-frequency components of the processed signals. In this way, the results of measurements can be enhanced as if the tests were performed in a faster TDR/TDT system (7).

TDR/TDT System Limitations

Most high-frequency TDR/TDT systems have been designed to investigate circuits whose impedance levels are close to 50 W. According to Ref. 2, 50-Ω systems are sufficiently accurate (<0.5% error) to measure load resistances or transmission-line characteristic impedances above 10 W. Testing changes of impedances or impedance profiling along the transmission channel, the lowest limit is 30 W to maintain errors below 1% (13).

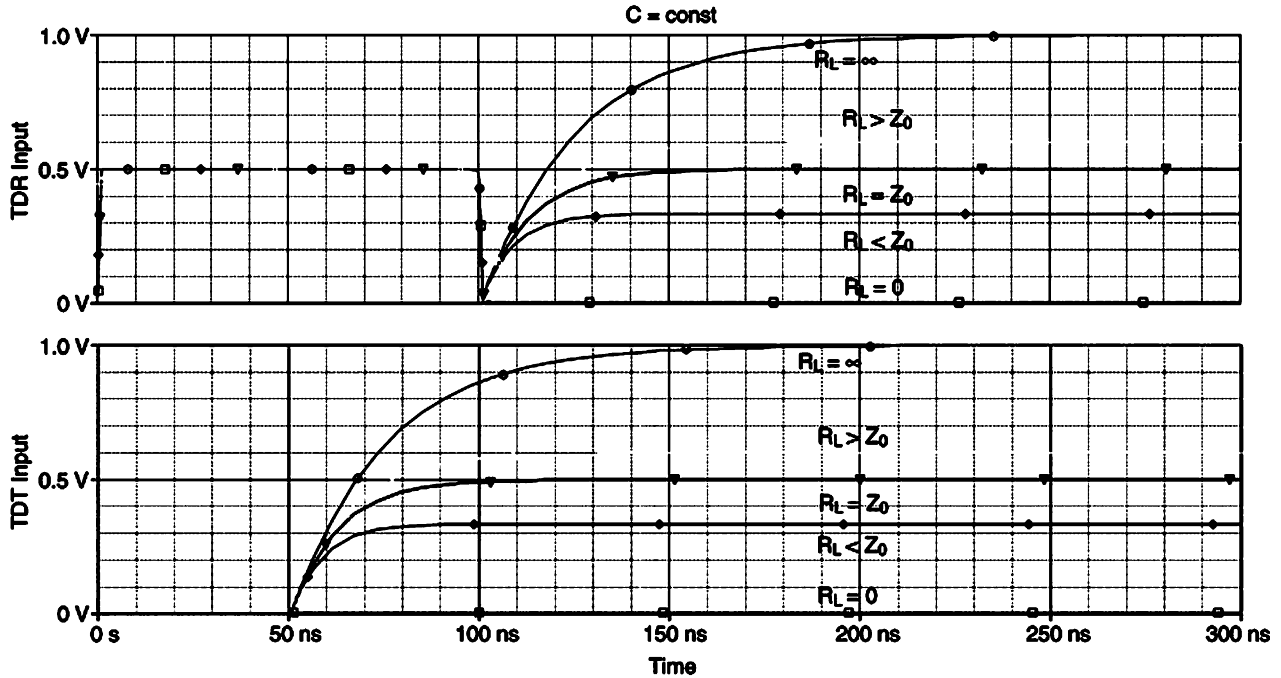

Figure 4. TDR input and TDT input voltages for parallel $R_{\mathrm{L}}C$ loads of the 50-Ω transmission-line test fixture.

The effects of the finite risetime of the TDR/TDT system limit the spatial resolution of the TDR measurements. The minimum distance that separates two consecutive discontinuities can be expressed as

$$\Delta d = \frac{c}{\sqrt{\varepsilon_{\mathrm{r}}}}\frac{t_{\mathrm{r}}}{4}$$

where t_{r} is the system risetime, c is the open-space wave velocity, and ε_{r} is the relative dielectric constant of the transmission-line dielectric (3). For instance, if the risetime is 20 ps and the relative dielectric constant is 2, then the minimum distance between two consecutive discontinuities is about 1 mm. This expression must be modified when the *jitter* is present in the measurement system. The jitter error has the same effect as if the equivalent risetime of the system had increased, thus reducing the spatial resolution.

System noise reduces the ability of TDR to detect small reflection amplitudes. Oscilloscope noise can reach the level of one division corresponding to maximum sensitivity of the scope (about 1 mV per division). Assuming that the incident pulse observed has an amplitude of 100 mV, reflection coefficients as small as 0.01 can be registered without major corruption caused by the noise. Better results can be achieved when analog smoothing or digital filtering is applied.

Differential Time-Domain Reflectometry

Differential time-domain reflectometry (DTDR) and reflectometers have been used to investigate symmetric transmission channels or lines such as *twisted-pair* or *slotted striplines* (8, 14). In DTDR systems, two pulses of opposite polarity are generated and applied to the tested symmetric DUT. Figure 14 shows a general block diagram for such a system. The *differential-mode impedance* can be determined from the reflections related to the differential input voltage, as shown in Fig. 15. The basic calculations are performed by the system processor, based on Eq. (2), and the results are displayed. *Common-mode impedance* can be also measured by using a single channel of the DTDR system (Fig. 16). The results obtained from Eq. (2) are multiplied by 2 if both transmission-line conductors are tested, as shown in Fig. 17. A drawback of differential TDR systems is that they require good pulse alignment. The errors introduced by misalignment can be reduced by means of normalization processes (8).

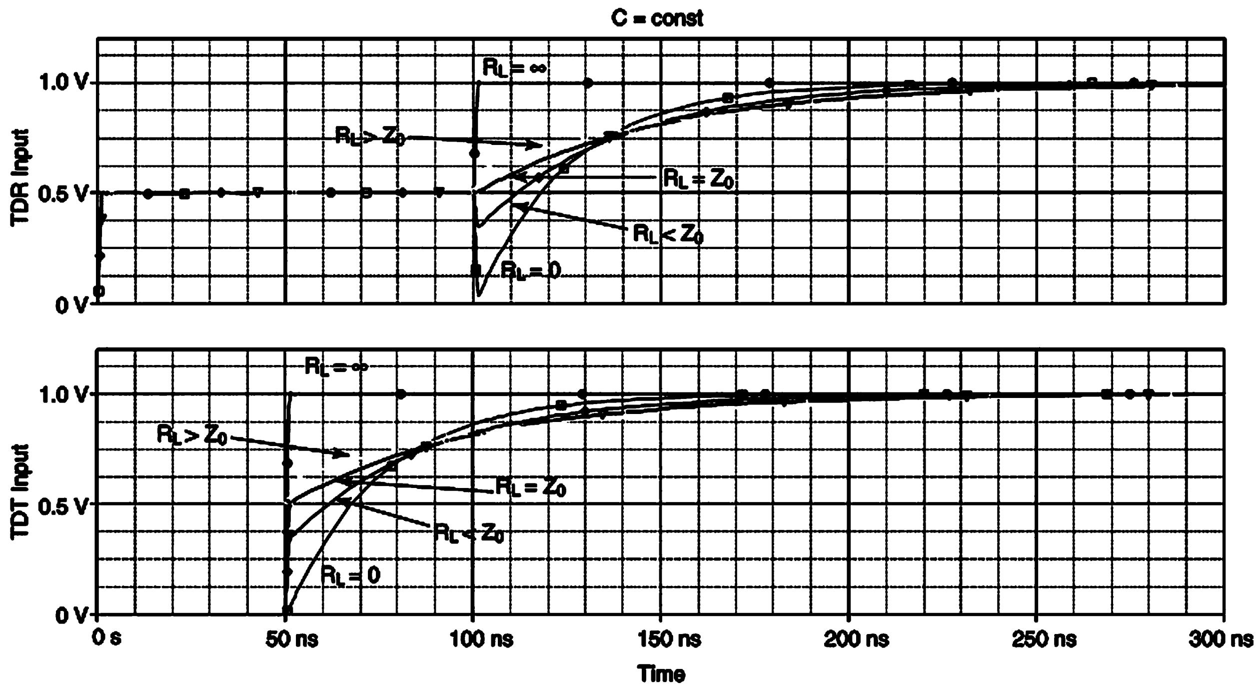

Figure 5. TDR input and TDT input voltages for series R_LC loads of the 50-Ω transmission-line test fixture.

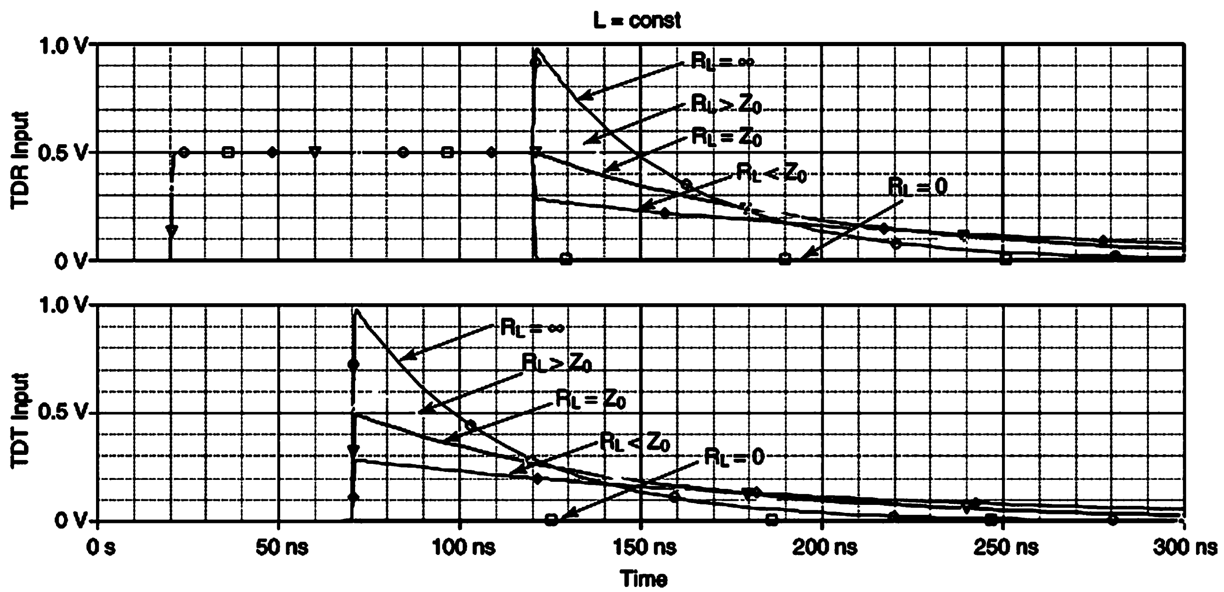

Figure 6. TDR input and TDT input voltages for parallel R_LL loads of the 50-Ω transmission-line test fixture.

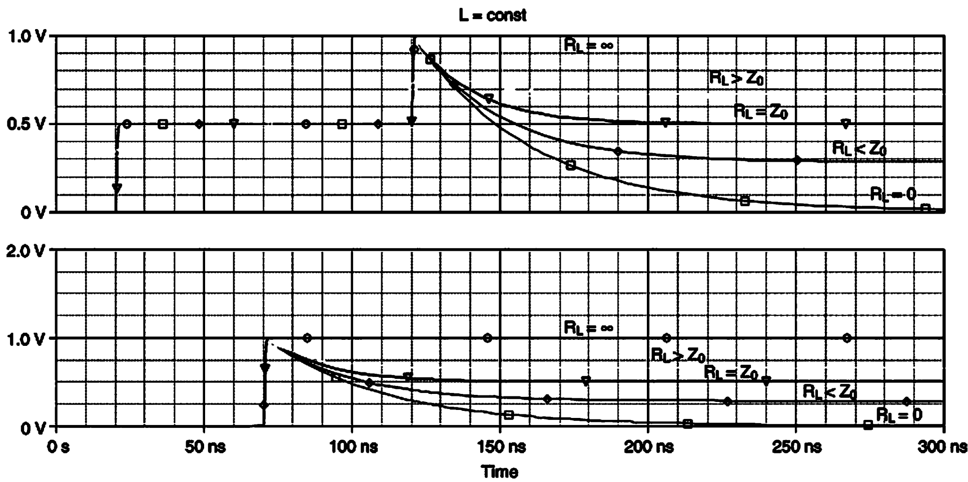

Figure 7. TDR input and TDT input voltages for series $R_L L$ loads of the 50-Ω transmission-line test fixture.

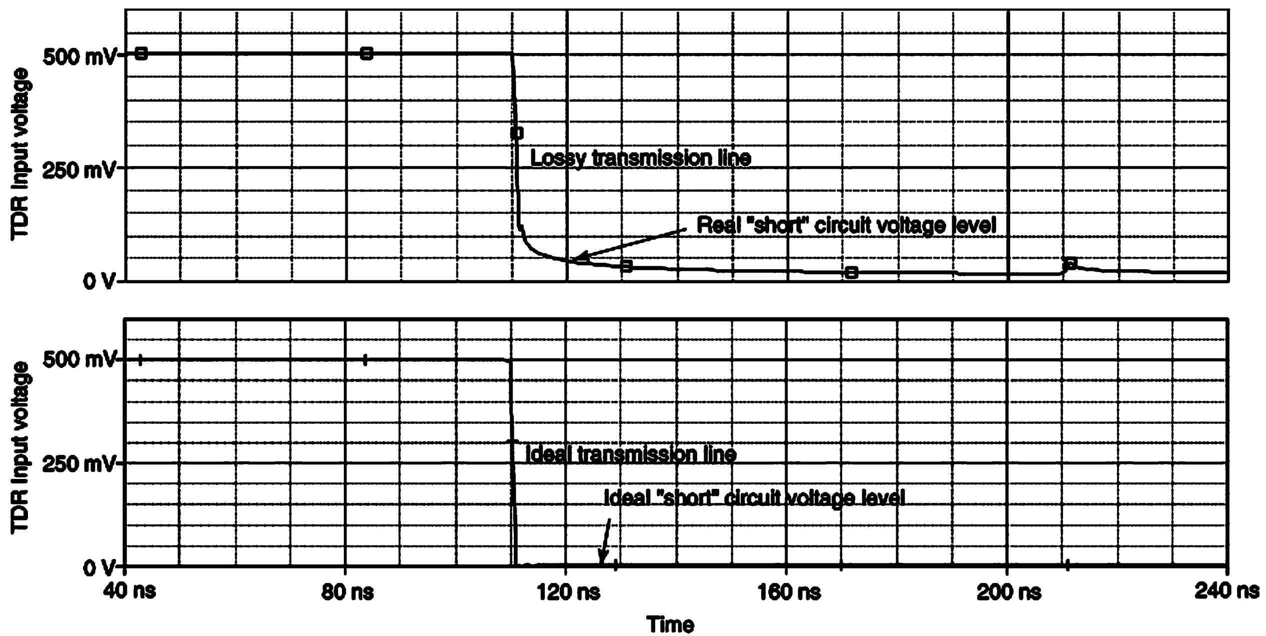

Figure 8. Reflected waves in short-ended transmission lines: (a) real transmission line; (b) ideal transmission line.

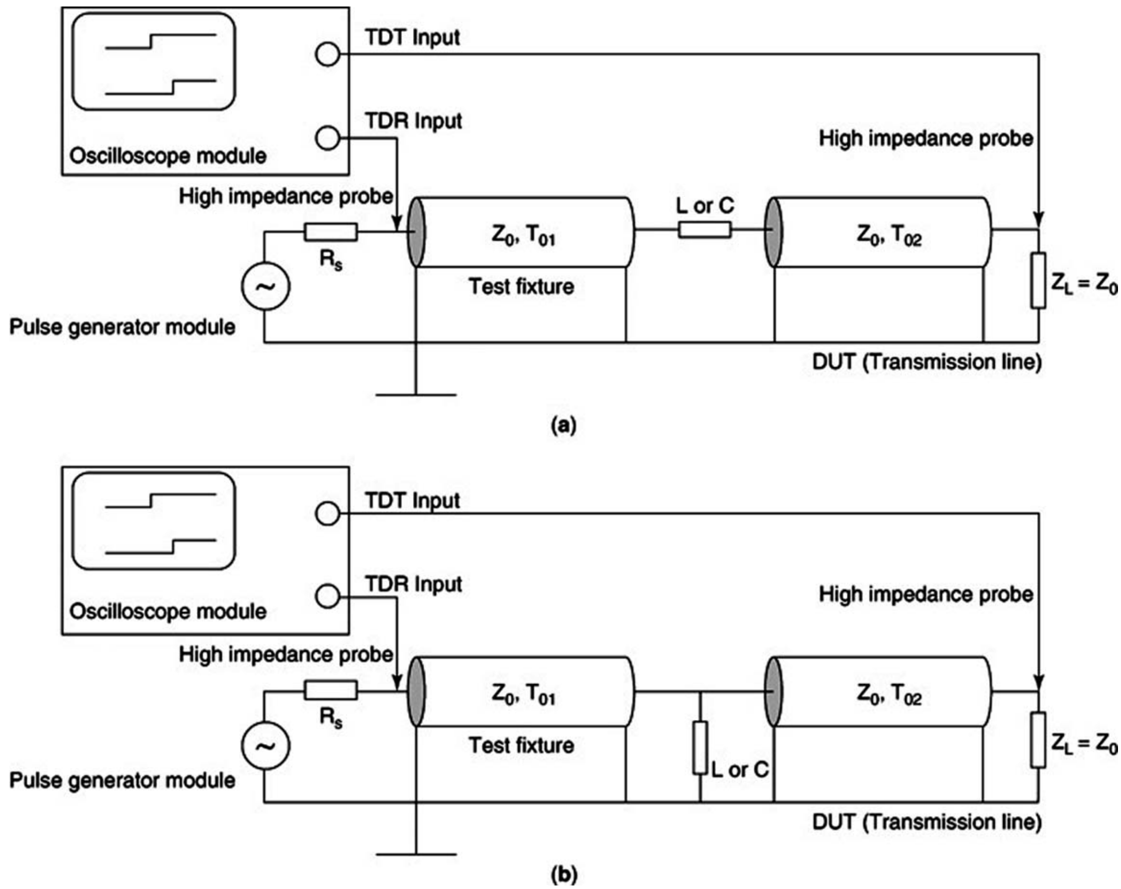

Figure 9. TDR/TDT tests of inserted reactance with a 50-Ω transmission-line test fixture: (a) series resistance; (b) parallel reactance.

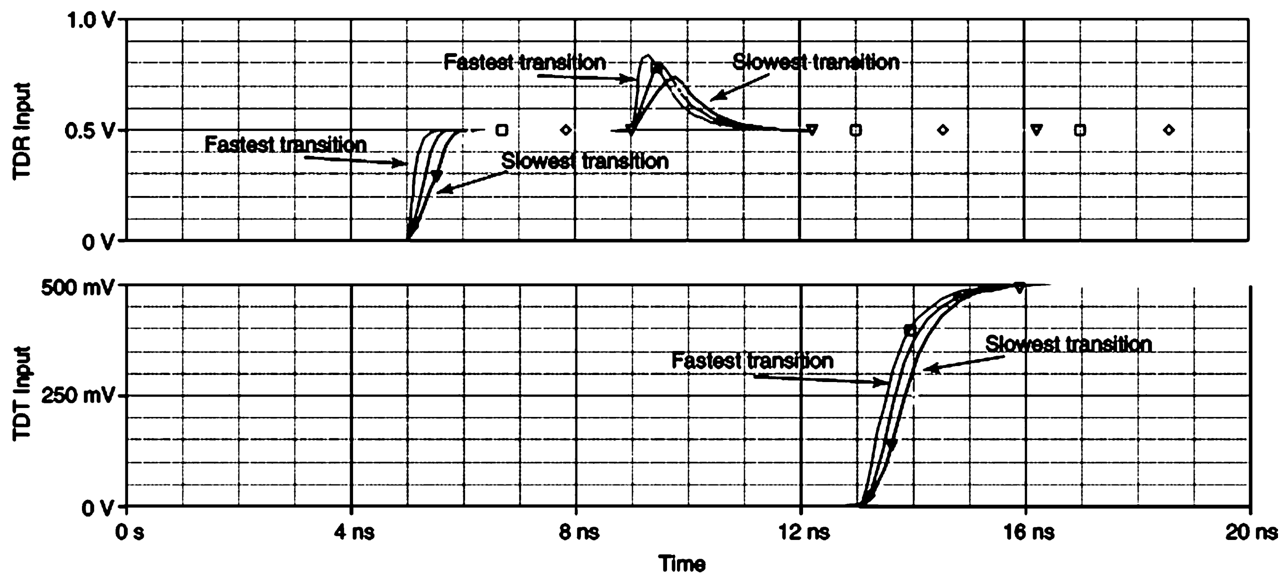

Figure 10. TDR and TDT input voltages for the system with an inductor inserted between transmission lines. Risetime of the input pulses is varied to show the distortion levels.

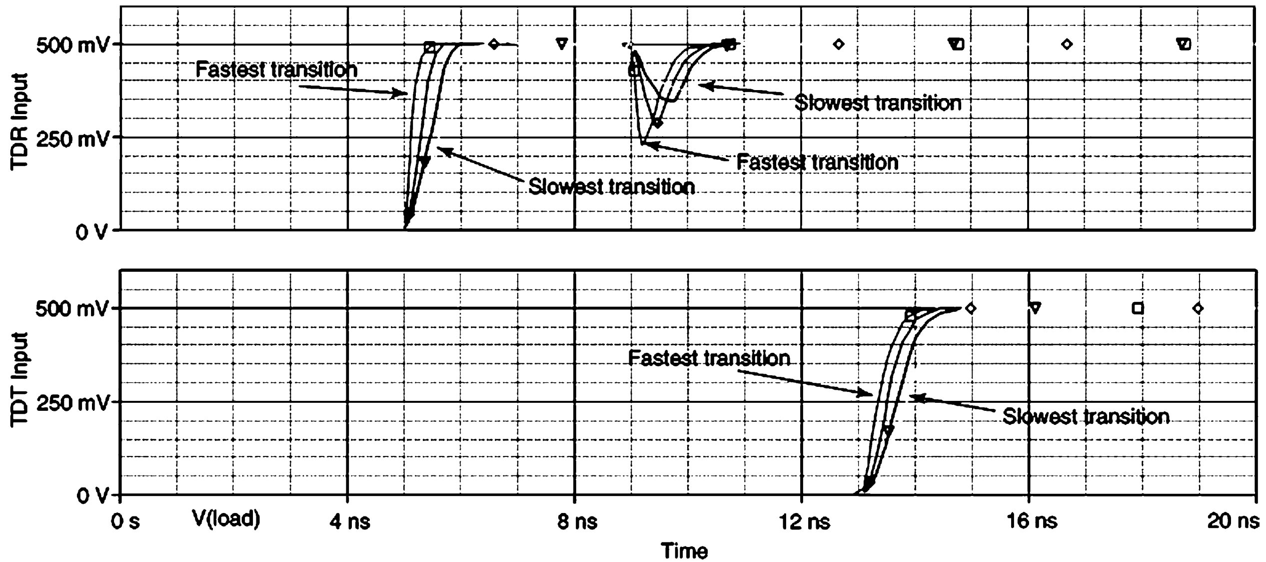

Figure 11. TDR and TDT input voltages for the system with a capacitor connected to the ground between transmission lines. Risetime of the input pulses is varied to show the distortion levels.

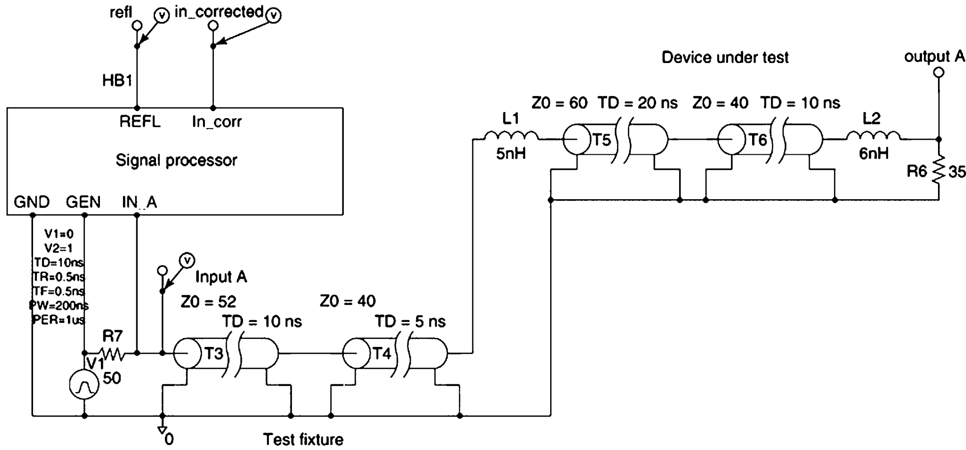

Figure 12. Simulated TDR/TDT system with imperfect test fixture.

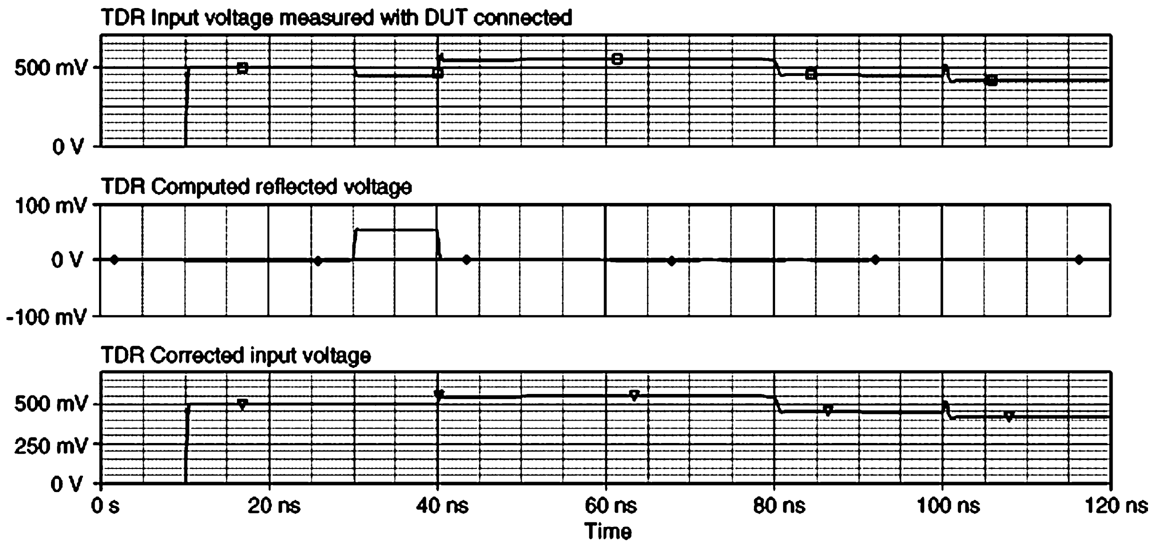

Figure 13. SPICE simulation results showing the effects of an imperfect test fixture and correction of its effect by subtraction.

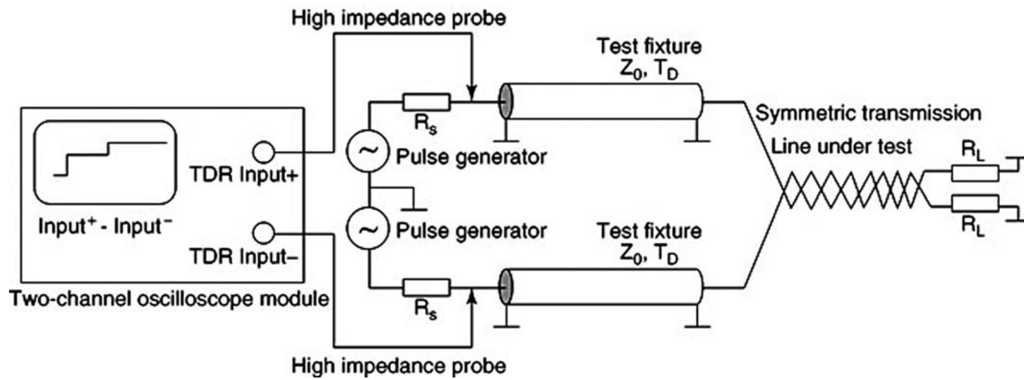

Figure 14. Differential impedance tests with a 50-Ω transmission-line test fixture.

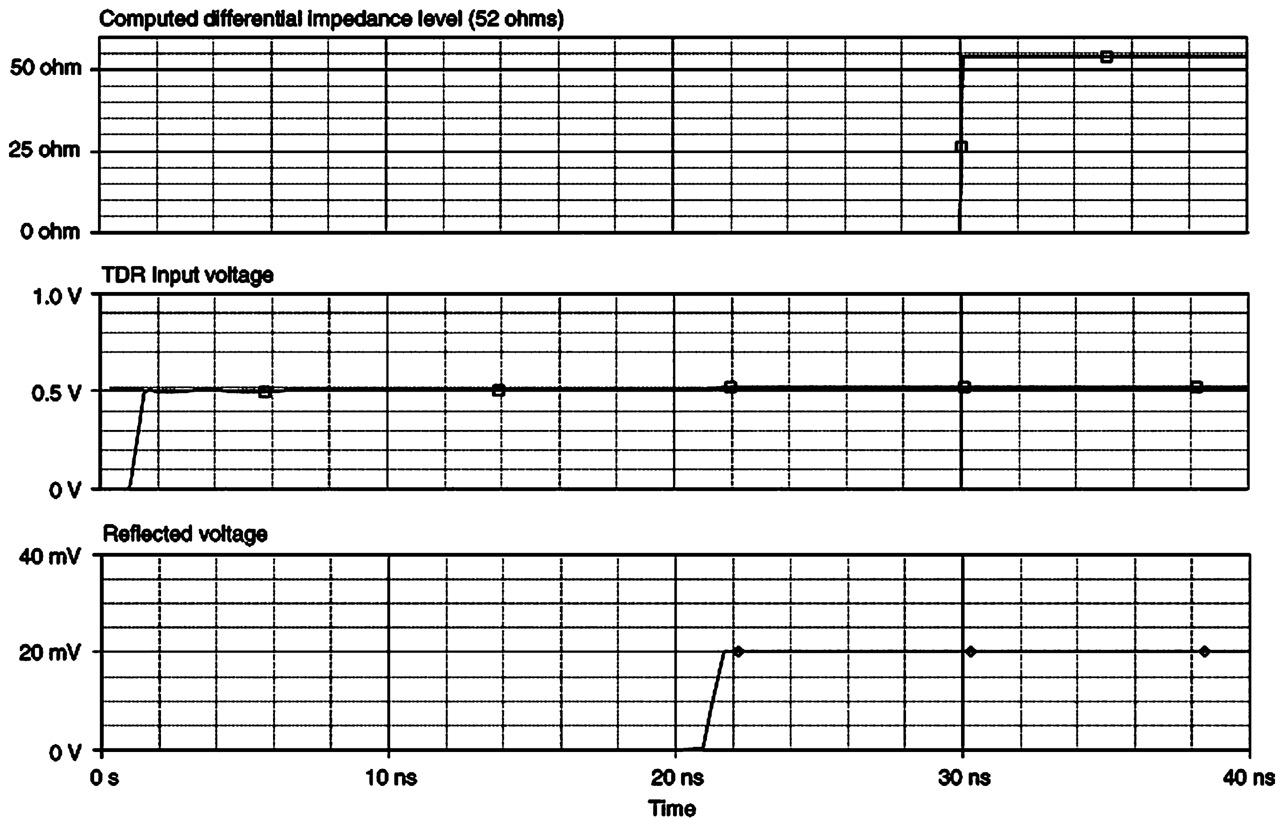

Figure 15. DTDR input, reflected voltages, and calculator output illustrating differential impedance measurement.

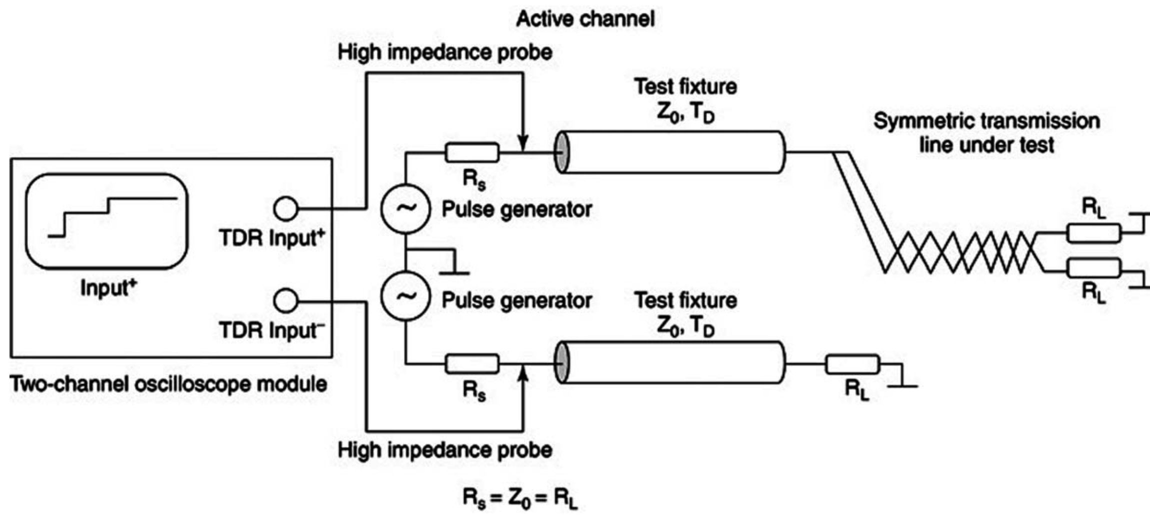

Figure 16. Single-channel measurement of a common-mode impedance with a 50-Ω transmission-line test fixture.

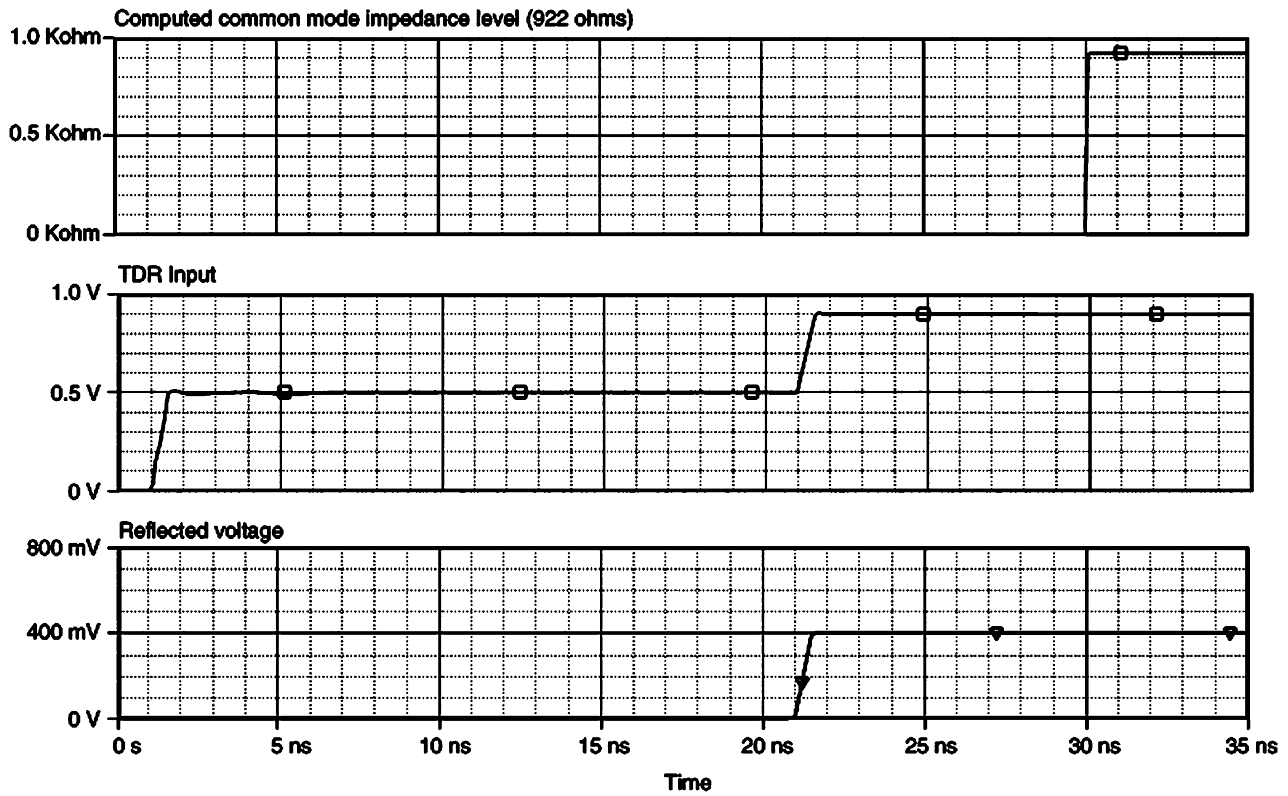

Figure 17. TDR measurement of common-mode impedance of symmetric transmission line.

EXAMPLES OF TDR/TDT TESTS AND TDR/TDT APPLICATIONS

TDR/TDT Test Examples

The following examples demonstrate the results of practical tests performed by a TDR/TDT measurement system (3, 4). Figure 18 shows the reflections observed when a long-lead resistor is connected to the end of a 50-Ω microstrip test fixture. The results from the measurement are displayed below the waveform. For example, the inductance of the resistor leads is 4.779448 nH, as the display shows. The next group of figures (Figs. 19,20,21) illustrate the process of normalization for a complex DUT. The test fixture was purposely selected to show the effectiveness of the normalization processes. The presence of the test fixture, which is normally used to delay unknown reflections with respect to the front of the test pulse, introduces visible signal distortions. The corrected measurements are shown in the last figure of this group. Normalization corrects for the effects of the test fixture and enhances the final reflections by shaping the reflections from the tested load as if faster testing pulses had been applied.

Figure 22 portrays the results from tests involving a hybrid power divider. The interaction between the two transmission-line branches introduces a crosstalk signal at point 2 of the tested board. The first reflection (point 1), with its level below the centerline of the scope screen, suggests that the initial, single section of the transmission line has a characteristic impedance greater than the impedance of the test fixture. The end terminations of the hybrid power divider introduce very small reflections due to lead inductances of the two resistors.

Application of TDR/TDT to Investigate Signal Integrity of High-Speed Circuits

Recently, increased data rates in communication and computer systems, often reaching subnanosecond switching speed, have created a need to introduce several gigabit standards and relate to them measurement methods. Conducting traces of the printed circuits, packaging connections, board connectors, and the connection of shorter or longer cables can degrade the *signal integrity* of the systems due to reflections, crosstalk, radiation, and losses in conductors and dielectrics. Application of the TDR/TDT measurement technique, combined with effective computer modeling, can help test the signal integrity of such systems during the initial design of circuit interconnections (16, 17). Figure 23 shows the composition for typical discontinuities connected between two sections of transmission lines, and Fig. 24 presents the corresponding TDR responses, which serve as basic signatures to help identify the types of discontinuities, find their structure, and, finally, determine the values of equivalent components.

In many practical systems, the TDR images are very complex because of the effects of *multiple reflections* caused by many discontinuities within the signal transmission channels. In such cases, hardware measurements can be enhanced by means of a computational method known as the *inverse scattering algorithm*, which was developed by TDA Systems Company (16, 17). To use such a technique, the *raw profile* of impedance is calculated from the input voltage data. Then the incident wave is computed from a reference TDR signal when a well-defined termination such as a short or open circuit is connected instead of the tested lines. The *true impedance profile* is then computed on the basis of the inverse scattering algorithm.

If a signal transmission forms a cascade of short sections of transmission lines of different impedances, the true impedance profile can be calculated from Eq. (2) by applying it to section junctions. A sequence of bouncing waves is assembled, and from the observed voltage levels, the re-

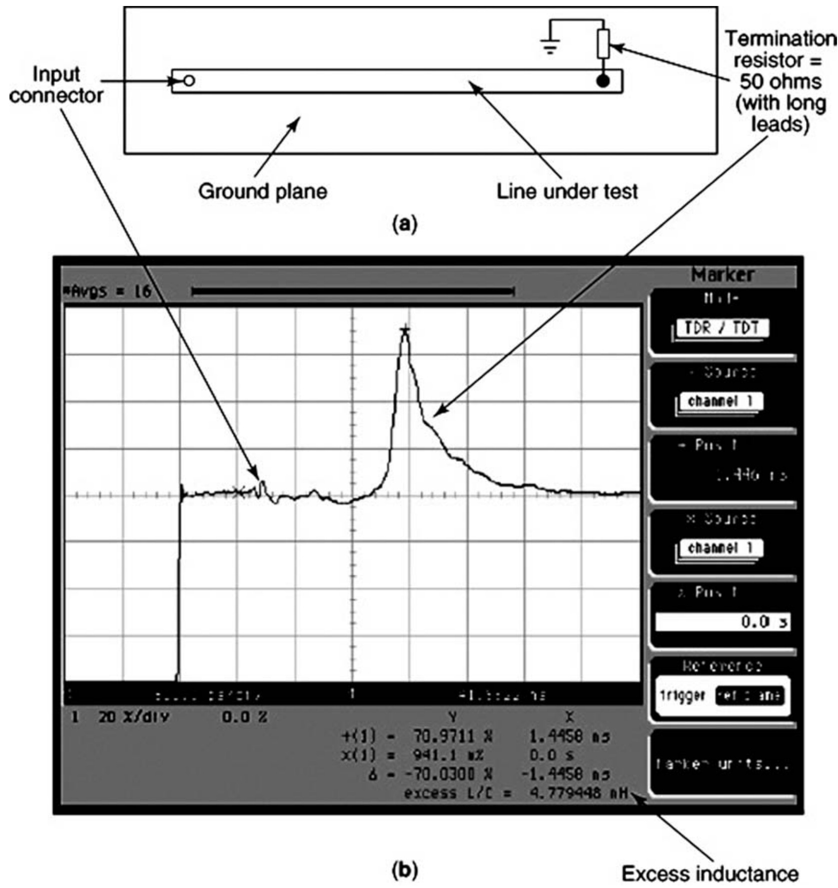

Figure 18. Effects due to termination resistor leads: (a) microstrip; (b) expanded TDR waveform (reprinted with permission of Agilent Technologies).

flection coefficients are calculated at each junction. Then Eq. (2) can be directly applied to find corresponding line impedances. Such processes are illustrated by means of Figs. 25,26,27. The reflections can be compared with simulation to increase the accuracy of the final modeling.

SUMMARY

This article has described the basic theory behind time-domain reflectometry. In addition, several practical aspects such as reflections and their analysis for resistive and nonresistive loads terminating transmission lines have been demonstrated. Both asymmetric and symmetric transmission-line TDR parameter tests have been also covered. Several practical oscilloscope displays have been included to illustrate normalization processes, which have been additionally reinforced by simulations. Finally, software-enhanced high-speed interconnect modeling was briefly discussed.

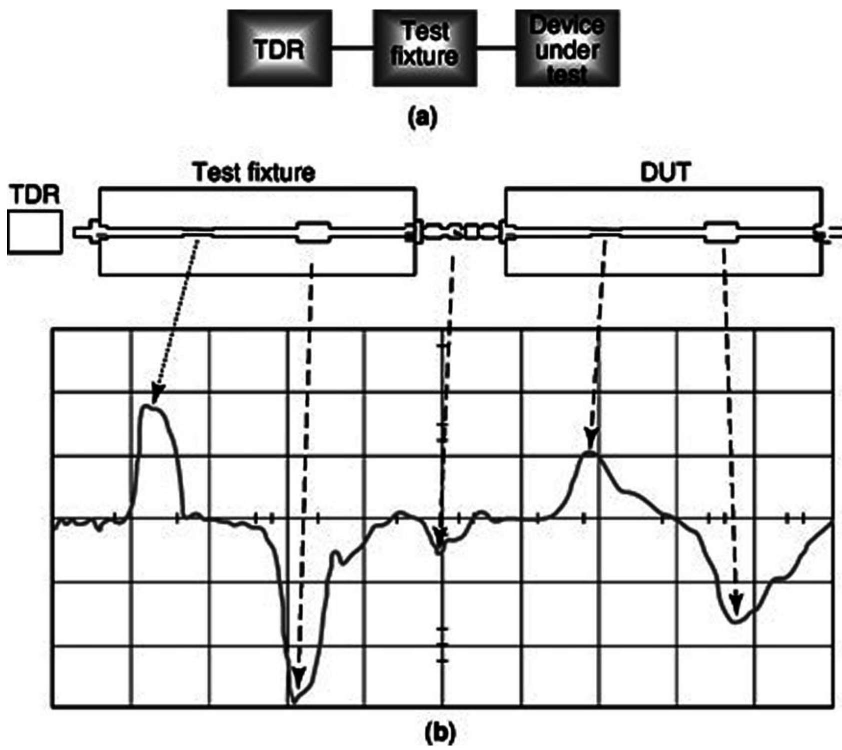

Figure 19. TDR measurements with the DUT at the end of imperfect test fixture: (a) block diagram; (b) unnormalized measurement results showing the effects of the test fixture (reprinted with permission of Agilent Technologies).

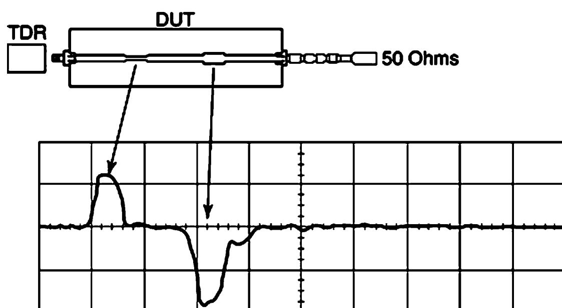

Figure 20. The unnormalized response of the DUT, measured without the test fixture (to demonstrate the results of normalization) (reprinted with permission of Agilent Technologies).

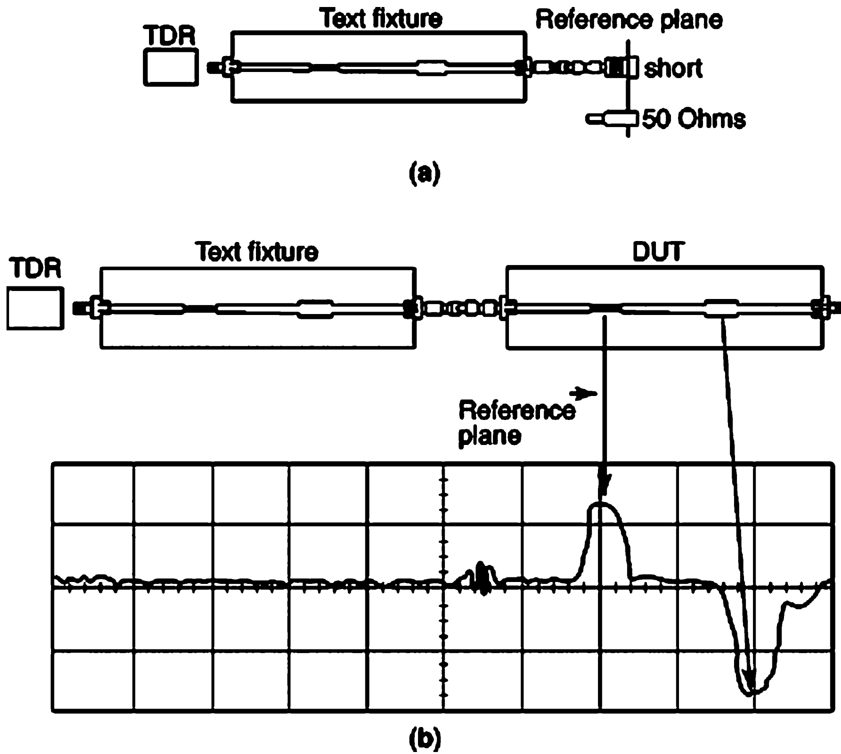

Figure 21. Normalized calibration that uses a short, then a 50-Ω termination to define a reference plane and generate a digital signature (filter): (a) circuit with the test fixture; (b) corrected measurements (reprinted with permission of Agilent Technologies).

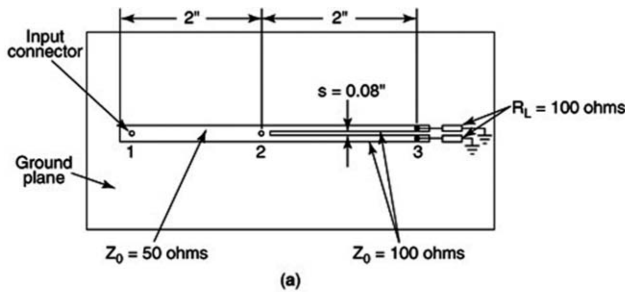

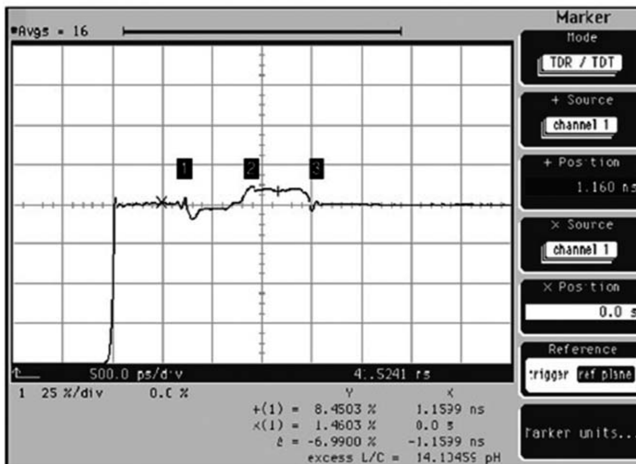

Figure 22. Example of the crosstalk in a hybrid power divider: (a) microstrip circuit; (b) expanded TDR waveforms (reprinted with permission of Agilent Technologies).

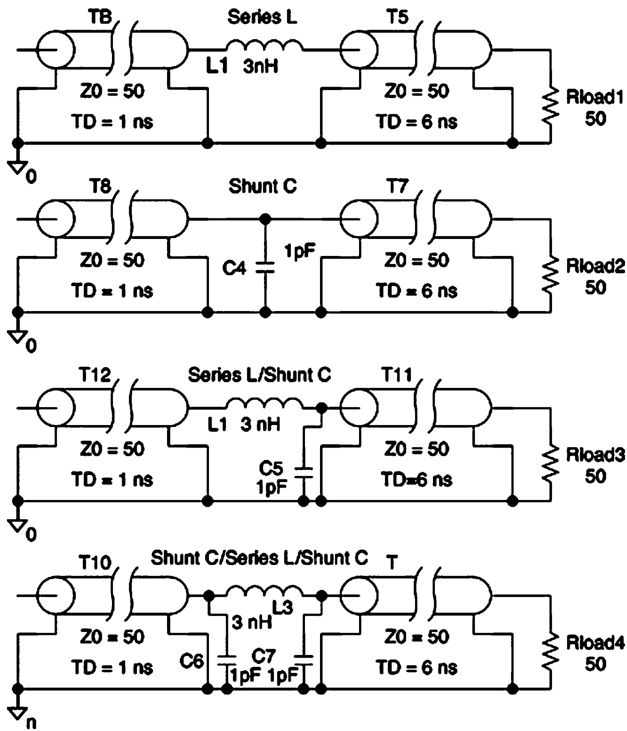

Figure 23. Typical examples of discontinuities represented in terms of lumped components.

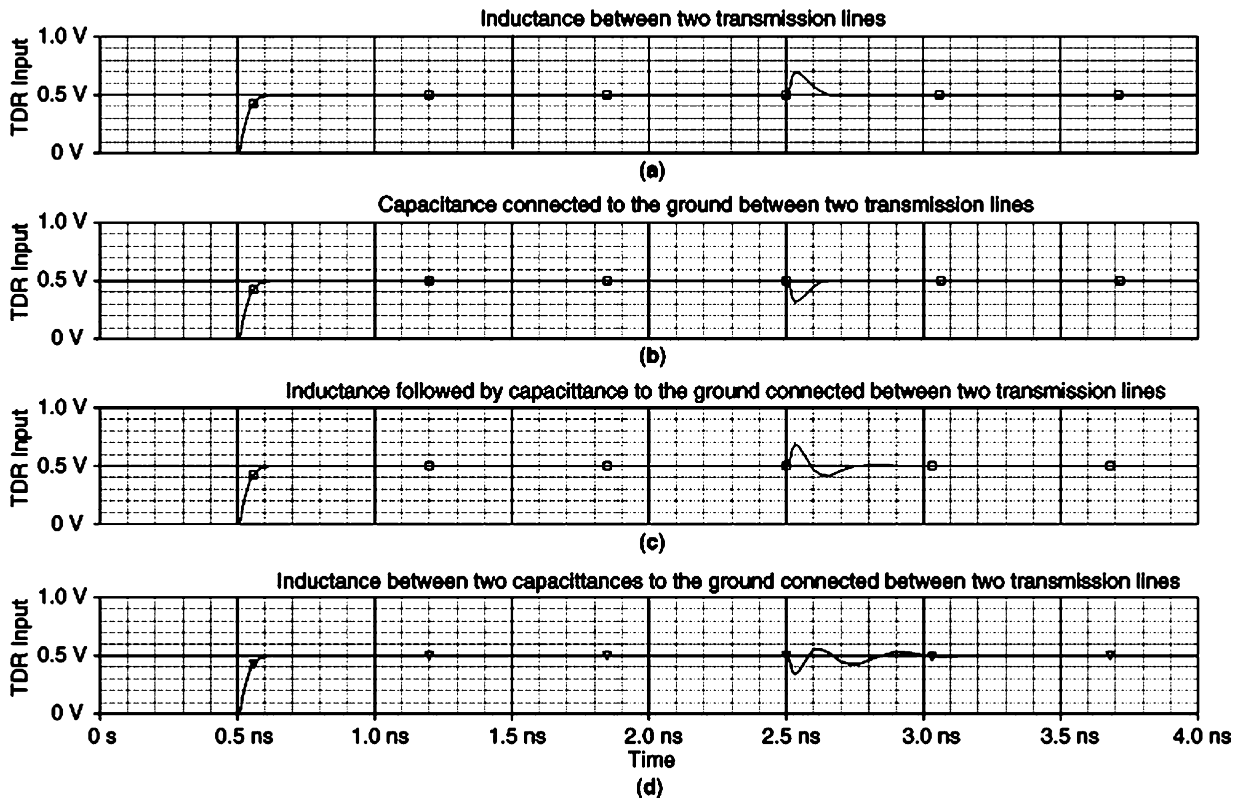

Figure 24. TDR input voltages observed in the circuit with two transmission lines and a reactance circuit inserted between them: (a) inductance between two transmission lines; (b) capacitance connected to the ground between two transmission lines; (c) inductance between two capacitances to the ground connected between two transmission lines.

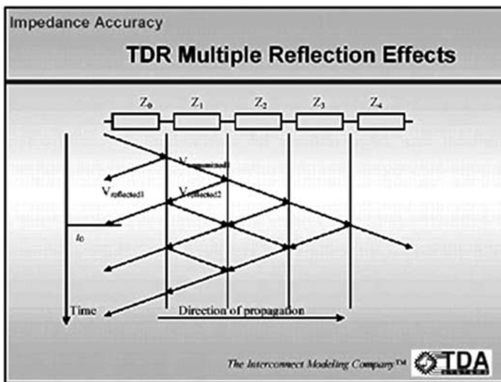

Figure 25. Bounced diagram for a cascade of transmission lines with different impedances (reproduced with permission of TDA Systems).

Impedance Accuracy

IConnect Computation of the True Impedance Profile

$$V_{reflected\,1} = \rho_1 V_{incident\,1}$$

$$V_{reflected\,2} = t_1^2 \rho_2 V_{incident\,1} + \rho_1 V_{incident\,2}$$

$$V_{reflected\,3} = (t_1^2 t_2^2 \rho_{32} - t_1^2 \rho_2^2 \rho_1) V_{incident\,1} + t_1^2 \rho_2 V_{incident\,2} + \rho_1 V_{incident\,3}$$

$$\begin{bmatrix} V_{reflected1} \\ V_{reflected2} \\ V_{reflected3} \\ \vdots \\ V_{reflectedn} \end{bmatrix} = \begin{bmatrix} k_1 & 0 & 0 & \cdots & 0 \\ k_2 & k_1 & 0 & 0 & 0 \\ k_3 & k_2 & k_1 & 0 & \vdots \\ \vdots & & & \ddots & 0 \\ k_n & k_{n-1} & k_{n-2} & \cdots & k_1 \end{bmatrix} \begin{bmatrix} V_{incident1} \\ V_{incident2} \\ V_{incident3} \\ \vdots \\ V_{incidentn} \end{bmatrix}$$

The Interconnect Modeling Company™ TDA

Figure 26. Expressions used to calculate the "true impedance profile" from the "raw impedance profile" using TDR input voltage levels (reproduced with permission of TDA Systems).

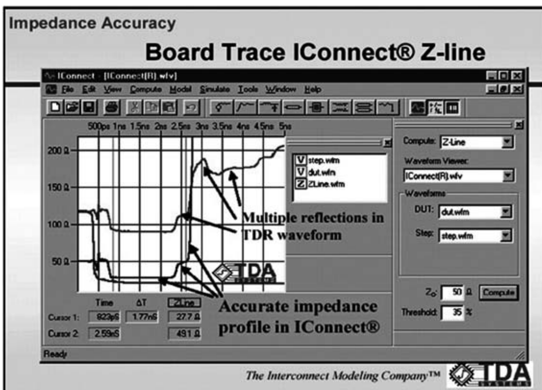

Figure 27. IConnect software application applied to determine the "true impedance profile" from the TDR voltages (reproduced with permission of TDA Systems).

BIBLIOGRAPHY

1. TDR Measurement of IEEE Implementation, homepage. (online): http://www.zayante.com/html/documentation/TDR %20Measurement%20whit.
2. N. G. Paulter, An assessment on the accuracy of time-domain reflectometry for measuring the characteristic impedance of transmission lines, *IEEE Trans. Instrum. Meas.* **50** (5): 300–303(Oct. 2001).
3. Agilent Technologies,Time Domain Reflectometry Theory,Application Note 1304-2.
4. Agilent Technologies,Evaluating Microstrip with Time-Domain Reflectometry, Application Note 1304-1.
5. Agilent Technologies,Improving TDR/TDT Measurement Using Normalization, Application Note 1304-5.
6. Hewlett-Packard,Advanced TDR Techniques, Application Note AN 62-3.
7. Agilent Technologies,Faster Risetime for TDR Measurements, Product Note 86100-4.
8. Agilent Technologies,Differential Impedance Measurement with Time Domain Reflectometry, Application Note 1382-5.
9. Tektronix Corporation,Users Manual of 1S2 Sampling Unit, Section 2.
10. D. J. Dasher, Measuring parasitic capacitance and inductance using TDR, *Hewlett-Packard J*. 83–96(April 1996).
11. Agilent Technologies,Agilent 86100B Wide-Band Oscilloscope, Technical Specifications.
12. Hewlett-Packard,Characterizing IC Packages with TDR/TDT and the UTP-3000 Test Fixture, Application Note 1210-5.
13. P. Ferrari and G. Angenieux, Calibration of a time-domain network analyzer: A new approach,<journalTitle>IEEE Trans. Instrum. Meas.</journalTitle> **49**(1): 178–187(Feb. 2000).
14. Hewlett-Packard,TDR Techniques for Differential Systems, Application Note 62-2.
15. PSPICE 9.1, homepage (online), OrCad: http://www.orcadpcb.com.
16. Signal Integrity Modeling of Gigabit Backplanes, Cables and Connectors Using TDR,TDA Application Note, 2002 (online), TDA Systems: http://www.tdasystems.com.
17. D. Smolyansky and S. D. Corey, High-speed digital interconnect modeling from TDR measurements,High-Performance System Design Conf., DesignCon 2000 (online), TDA Systems: http://www.tdasystems.com.

ANDREW RUSEK
Oakland University, Rochester, MI